NATIONAL AERONAUTICS AND SPACE ADMINISTRATION

TECHNICAL MEMORANDUM X-610

STATIC LONGITUDINAL AERODYNAMIC CHARACTERISTICS AT TRANSONIC SPEEDS AND ANGLES OF ATTACK UP TO 99° OF A REENTRY GLIDER HAVING FOLDING WING-TIP PANELS*

By Walter B. Olstad

SUMMARY

Data are presented which were obtained from a transonic wind-tunnel investigation of a reentry glider having folding wing-tip panels. The tests were conducted at angles of attack from -4° to 99°. The Reynolds number based on the mean geometric chord of the fixed planform varied from 2.35×10^6 to 2.99×10^6.

The maximum lift-drag ratio for the model with the folding wing-tip panels fully extended decreased from a maximum value of 7.8 at a Mach number of 0.60 to about 3.4 at Mach numbers from 1.03 to 1.20. The model with the folding wing panels fully extended was stable for values of the lift coefficient from 0 up to at least 0.8. Above this lift coefficient pitch-up tendencies were observed, followed by an unstable or neutrally stable region which extended up to values of angle of attack of 50° or 60°. Deflecting the folding wing panels between 45° and 90° (fully retracted) would be ineffective in producing a significant change in the trim angle of attack or in any of the force or moment coefficients in the angle-of-attack range from 49° to 99°.

INTRODUCTION

A variety of configurations have been proposed as hypersonic boost-glide and/or atmospheric reentry vehicles. Generally, the primary design considerations were reduced heat transfer and acceptable flying characteristics at hypersonic speeds. However, these vehicles must also have acceptable flying characteristics at lower speeds. Therefore, an extensive program has been undertaken at the Langley Research Center to study

*Title, Unclassified.

the aerodynamic characteristics at subsonic to hypersonic speeds of many of these configurations. Since some of these vehicles may traverse a large portion of the flight path at high angles of attack, these studies generally cover a wide angle-of-attack range. Transonic tests of five of these vehicles in the general program are reported in references 1 to 5. The results of an investigation of the static longitudinal aerodynamic characteristics of another configuration are reported herein.

The configuration investigated herein consists of a clipped delta wing with leading edges swept back 76° and the fuselage mounted on the upper surface of the wing. Folding wing-tip panels are located near the rear of the vehicle. During the initial stages of reentry the vehicle would operate at angles of attack near 90° with the folding wing panels fully retracted from the airstream. At low supersonic speeds or subsonic speeds these wing panels would be extended in order to add planform area behind the center of gravity of the vehicle and thus trim the vehicle to lower angles of attack for efficient gliding. A more complete discussion of this configuration as a manned reentry vehicle is presented in reference 6. Some results of investigations of similar models at subsonic and supersonic speeds are presented in references 7 to 10.

L 1 6 5 1

Tests were conducted at Mach numbers from 0.60 to 1.20 and angles of attack from -4° to 99°. Reynolds number based on the mean geometric chord of the fixed planform varied from 2.35×10^6 to 2.99×10^6.

SYMBOLS

The force and moment coefficients are referred to the wind and body axes systems with the origin located longitudinally at 50 percent of the mean geometric chord of the fixed planform and vertically 7.3 percent of the mean geometric chord above the wing chord plane. All force and moment coefficients are based on the fixed wing planform area.

C_L lift coefficient, $\frac{\text{Lift}}{q_\infty S}$

C_{L_α} slope of the lift curve, $\frac{\partial C_L}{\partial \alpha}$

C_N normal-force coefficient, $\frac{\text{Normal force}}{q_\infty S}$

C_D	drag coefficient, $\frac{\text{Drag}}{q_\infty S}$
C_A	axial-force coefficient, $\frac{\text{Axial force}}{q_\infty S}$
C_m	pitching-moment coefficient, $\frac{\text{Pitching moment about } 0.50\bar{c}}{q_\infty S\bar{c}}$
C_{m_α}	slope of the pitching-moment curve, $\frac{\partial C_m}{\partial \alpha}$
$C_{p,b}$	balance-chamber pressure coefficient, $\frac{p_b - p_\infty}{q_\infty}$
$\bar{c}$	mean geometric chord of the fixed planform area
p_b	static pressure in the model balance chamber
p_∞	free-stream static pressure
q_∞	free-stream dynamic pressure
$\frac{L}{D}$	lift-drag ratio
M	free-stream Mach number
R	Reynolds number based on $\bar{c}$
r	radius
S	fixed wing planform area
α	angle of attack
δ	deflection angle of folding wing panels ($\delta = 0^\circ$ when wing panels fully extended; see fig. 1(a))

Subscripts:

max	maximum
min	minimum
$(L/D)_{max}$	at maximum lift-drag ratio

APPARATUS AND TESTS

Tunnel

The tests were conducted in the Langley 8-foot transonic pressure tunnel which is a rectangular, slotted-throat, single-return tunnel designed to obtain aerodynamic data at transonic speeds while minimizing the effects of choking and blockage. Details of the tunnel are presented in reference 11.

Model

Details of the model are presented in figure 1 and table I. Photographs of the model are presented in figure 2.

The fixed wing of the model was a clipped delta wing with leading edges swept back 76°. The airfoil section was generated by cutting away 8.72 percent of the resultant mean geometric chord from the leading and trailing edges of a 3-percent-thick circular-arc airfoil. The leading edge was rounded and the trailing edge was blunt. The tip of the wing was clipped so that the actual model wing had an aspect ratio of 0.73.

The folding wing-tip panels were unswept and had a taper ratio of 0.76. (See fig. 1(b).) The panels had an NACA 6306 airfoil section which was inclined at an incidence angle of -6° with the chord plane of the fixed wing when the deflection angle of the wing panels was zero. The midchord line of the folding wing panels for $\delta = 0°$ (wing panels horizontal) was held 12.72 percent $\bar{c}$ above the chord plane of the fixed wing by means of a vertical strut. With the folding wing panels at a deflection angle of 0°, the aspect ratio of the exposed planform was 2.25. The folding wing panels were set at deflection angles of 0°, 15°, 45°, and 90° during this investigation.

The fuselage was mounted on the wing upper surface so that it would be completely shielded from the free stream at angles of attack near 90°. A delta-planform vertical tail was mounted on the rearward portion of the fuselage. Two forward and two rearward control vanes were mounted on the model in their fully retracted positions. The position of these vanes was not changed during the investigation. These vanes are used for control when the folding wing panels of the vehicle are completely retracted ($\delta = 90°$).

Model Support Systems

A three-component internal strain-gage balance was attached to the forward end of the conventional straight sting and was housed within

the model. At angles of attack from -4° to 39° the model was supported by the sting which extended from the model base and was attached to the central support system of the tunnel. (See figs. 1(a) and 2(a).) A 30° angle coupling was inserted in the system behind the sting (approximately 42 inches behind the base of the model) in order to obtain angles of attack from 20° to 39°. At angles of attack from 49° to 99° an adapter was attached to the forward end of the sting. (See figs. 1(c), 2(b), and 2(c).) Use of this high-angle adapter necessitated the removal of the vertical tail. The adjustable adapter, which was attached to the balance, was fixed at angles of 60° and 80°, and the angle of attack of the model was varied about these settings by varying the angle of the central support system.

Tests

Tests of the model were made at Mach numbers from 0.60 to 1.20. The folding wing-tip panels were set at deflection angles of 0°, 15°, 45°, and 90° during this investigation. The angle-of-attack range investigated for each deflection angle is given in the following table:

Deflection angle, δ, deg	Angle-of-attack range, deg
0	-4 to 99
15	18 to 99
45	49 to 99
90	49 to 99

These angle-of-attack ranges apply throughout the complete Mach number range.

Tests were made at a stagnation pressure of approximately 2/3 atmosphere. Therefore, the Reynolds number based on the wing mean geometric chord varied during this investigation from about 2.35×10^6 to 2.99×10^6. (See fig. 3.)

No attempt was made to fix transition during these tests.

Measurements and Accuracy

Model forces and moments were measured with an internally mounted three-component strain-gage balance. The angle of attack was measured

with a strain-gage attitude transmitter mounted in the tunnel central support tube and was adjusted for flow angularity and balance and sting deflections under load. The pressure in the balance chamber was measured by an orifice located within the chamber about 4.5 inches forward of the model base.

The coefficients are estimated to be accurate within the following limits:

M	Accuracy of -			
	C_N	C_A	C_m	$C_{p,b}$
0.60	±0.037	±0.003	±0.007	±0.02
1.20	±.018	±.001	±.004	±.02

The angle of attack is estimated to be accurate within ±0.1°. The average free-stream Mach number was held to within ±0.005 of the nominal values presented in this paper.

Corrections

No corrections have been applied to the data for boundary-interference effects. At subsonic speeds, the slotted test section minimized boundary-interference effects such as blockage and boundary-induced upwash. No test data were obtained for Mach numbers between 1.03 and 1.13 because the supersonic boundary-reflected disturbances impinged on the model within this range. At Mach numbers of 1.03 and below, the magnitudes of the disturbances were negligible.

The effects of the presence of the support systems were not determined during these tests, and no corrections have been applied to the data to account for support interference.

The axial-force and drag coefficients presented herein have not been adjusted to free-stream conditions at the model base.

RESULTS AND DISCUSSION

The variation of the balance-chamber pressure coefficient with angle of attack is presented in figure 4. The longitudinal aerodynamic characteristics of the model are presented in figure 5. Figures 6, 7, and 8 present analysis curves for the model. The values of C_{m_α}

presented in figure 6 represent the instantaneous slopes at the values of angle of attack corresponding to lift coefficients of 0.2, 0.4, and 0.6. The values of lift-curve slope shown in figure 6 represent average slope over a range of lift coefficients from 0 to 0.4. The slopes in figure 8 were taken as average slopes over a small angle range near an angle of attack of 90°. The other quantities in figures 6 to 8 were obtained from the faired curves of figure 5.

Support-System Interference

L
1
6
5
1

The results of references 3 to 5 indicate a difference in support-system interference on the model when the model was mounted on the conventional straight sting and when it was mounted on the high-angle adapter. It was shown that the model when mounted on the conventional straight sting should be more nearly interference free at low angles of attack ($\alpha < 34^\circ$), whereas the model mounted on the high-angle adapter should suffer less from interference effects at high angles of attack ($\alpha > 60^\circ$). The differences in interference effects for the two support systems were shown to have a large effect on the balance-chamber pressure coefficients and a smaller though significant effect on the force and moment coefficients in the angle-of-attack range from 20° to 34°, where data for the two systems were available. It seems likely that the model of the present investigation would be similarly affected by the different support systems. However, no data are available over a common angle-of-attack range, so the magnitudes of the difference in support-system interference for the two systems is unknown. For this reason, no attempt was made to connect by a faired curve the data points for the model when mounted on the two different support systems.

Aerodynamic Characteristics of the Model

The lift curves for the model with the folding wing panels fully extended ($\delta = 0^\circ$) appeared to be linear for values of the lift coefficient from 0 to 0.6 throughout the Mach number range. (See fig. 5(a).) The value of the lift-curve slope (see fig. 6) varied from a subsonic level of 0.051 to about 0.057 at Mach numbers between 1.13 and 1.20. The angle of attack at which the lift coefficient was a maximum was about 40° for all the test Mach numbers (fig. 5(a)). The value of the maximum lift coefficient for the model with the folding wing panels fully extended varied from a minimum of about 1.08 to a maximum of about 1.33. Retraction of the folding wing panels tended to reduce the values of maximum lift coefficient. Near an angle of attack of 90° the lift curves appeared to be linear for all values of the folding wing panel deflection angle δ. Figure 8 indicates that the slope of the lift curve near an angle of attack of 90° was more negative for the model with

folding wing panels fully extended ($\delta = 0^\circ$) than with the panels fully retracted ($\delta = 90^\circ$). The variation of lift-curve slope with Mach number for the two configurations was similar.

The minimum-drag curve for the model with the folding wing panels fully extended (fig. 6) exhibited typical transonic drag-rise characteristics. At an angle of attack of 90° the transonic drag rise was again evident for the model with the folding wing panels fully extended and fully retracted. (See fig. 8.) Extending the wing panels increased the drag about 25 percent throughout the Mach number range at an angle of attack of 90°. The maximum lift-drag ratio for the model with the folding wing panels fully extended decreased from a maximum value of 7.8 at $M = 0.60$ to about 3.4 at $M = 1.03$ to $M = 1.20$. (See fig. 7.) The lift coefficient for maximum lift-drag ratio varied over the Mach number range from 0.30 to 0.58, and the angle of attack for maximum lift-drag ratio varied from 5.5° to 11.2°. Retracting the folding wing panels had no apparent effect on the lift-drag ratio (fig. 5(f)) for the range of Mach numbers and angles of attack investigated.

The model with the folding wing panels fully extended was stable for values of lift coefficient from 0 up to at least 0.80 (corresponding to angles of attack from approximately 0° to 15°) for all test Mach numbers. (See figs. 5(c) and 6.) In this region the pitching-moment curves were smooth, though not always linear. At lift coefficients slightly in excess of 0.80 a pitch-up tendency was evident. The severity of this pitch-up tendency was greatest at the lowest test Mach number of 0.60. These pitch-up tendencies were followed by an unstable or neutrally stable region. The model was generally unstable or neutrally stable near the angle of attack for maximum lift coefficient. From an angle of attack of 50° or 60° (depending on Mach number) to 99° the model was stable. Retracting the folding wing panels produced a positive increment in the pitching-moment coefficients but had only a small effect on the stability level throughout the Mach number and angle-of-attack ranges. (See figs. 5(c) and 8.) Deflecting the folding wing panels between $\delta = 45^\circ$ and $\delta = 90^\circ$ (fully retracted) proved ineffective in producing a significant change in the trim angle of attack or in any of the force or moment coefficients in the angle-of-attack range from 49° to 99° (fig. 5).

CONCLUSIONS

Analysis of data from tests at transonic speeds and angles of attack from -4° to 99° on a reentry glider having folding wing-tip panels has led to the following conclusions:

1. The maximum lift-drag ratio for the model with the folding wing panels fully extended decreased from a maximum value of 7.8 at a Mach number of 0.60 to about 3.4 at Mach numbers from 1.03 to 1.20.

2. The model with the folding wing panels fully extended was stable for values of the lift coefficient from 0 up to at least 0.80. Above this lift coefficient pitch-up tendencies were observed followed by an unstable or neutrally stable region which extended up to values of angle of attack of 50° or 60°.

L
1
6
5
1

3. Deflecting the folding wing panels between 45° and 90° (fully retracted) would be ineffective in producing a significant change in the trim angle of attack or in any of the force or moment coefficients in the angle-of-attack range from 49° to 99°.

Langley Research Center,
National Aeronautics and Space Administration,
Langley Air Force Base, Va., August 31, 1961.

[redacted]

REFERENCES

1. Mugler, John P., Jr., and Olstad, Walter B.: Static Longitudinal Aerodynamic Characteristics at Transonic Speeds of a Lenticular-Shaped Reentry Vehicle. NASA TM X-423, 1960.

2. Olstad, Walter B., Mugler, John P., Jr., and Cahn, Maurice S.: Static Longitudinal and Lateral Stability Characteristics of a Right Triangular Pyramidal Lifting Reentry Configuration at Transonic Speeds. NASA TN D-655, 1961.

3. Olstad, Walter B., and Mugler, John P., Jr.: Static Longitudinal Aerodynamic Characteristics at Transonic Speeds of a Thick Delta-Wing Hypersonic-Glider Configuration for Angles of Attack up to 100°. NASA TM X-532, 1961.

4. Mugler, John P., Jr., and Olstad, Walter B.: Static Longitudinal Aerodynamic Characteristics at Transonic Speeds of a Blunted Right Triangular Pyramidal Lifting Reentry Configuration for Angles of Attack up to 110°. NASA TN D-797, 1961.

5. Olstad, Walter B.: Static Longitudinal Aerodynamic Characteristics at Transonic Speeds of a Flat Delta-Wing Hypersonic Glider for Angles of Attack up to 100°. NASA TM X-557, 1961.

6. Staff of Langley Flight Research Division (Donald C. Cheatham, compiler): A Concept of a Manned Satellite Reentry Which Is Completed With a Glide Landing. NASA TM X-226, 1959.

7. Foster, Gerald V.: Exploratory Investigation at Mach Number of 2.01 of the Longitudinal Stability and Control Characteristics of a Winged Reentry Configuration. NASA TM X-178, 1959.

8. Spencer, Bernard, Jr.: High-Subsonic-Speed Investigation of the Static Longitudinal Aerodynamic Characteristics of Several Delta-Wing Configurations for Angles of Attack From 0° to 90°. NASA TM X-168, 1959.

9. Spencer, Bernard, Jr.: An Investigation at Subsonic Speeds of Aerodynamic Characteristics at Angles of Attack From -4° to 100° of a Delta-Wing Reentry Configuration Having Folding Wingtip Panels. NASA TM X-288, 1960.

10. Spencer, Bernard, Jr.: An Investigation at Subsonic Speeds of the Longitudinal Aerodynamic Characteristics at Angles of Attack From -4° to 100° of Delta-Wing Reentry Configurations Having Vertically Displaced and Cambered Wingtip Panels. NASA TM X-440, 1961.

[redacted]

11. Mugler, John P., Jr.: Transonic Wind-Tunnel Investigation of the Aerodynamic Loading Characteristics of a 60° Delta Wing in the Presence of a Body With and Without Indentation. NACA RM L55G11, 1955.

TABLE I

MODEL DIMENSIONS

Center-of-gravity location:	
Longitudinal, in. from nose	10.49
Longitudinal, percent $\bar{c}$	0.50
Vertical, in. above wing chord plane	0.92
Fixed clipped delta wing:	
Airfoil section	Circular arc with blunted and rounded leading edge and blunted trailing edge
Area, sq ft	0.578
Span, in.	7.80
Mean geometric chord, $\bar{c}$, in.	12.62
Aspect ratio	0.73
Taper ratio	0.178
Distance of $\bar{c}$ from body longitudinal axis, in.	1.49
Folding wing panels:	
Airfoil section	NACA 6306
Area (both panels), sq ft	0.156
Total exposed area (fixed wing plus panels at $\delta = 0^{\circ}$), sq ft	0.721
Total exposed span (fixed wing plus panels), in.	15.28
Total exposed aspect ratio (fixed wing plus panels)	2.25

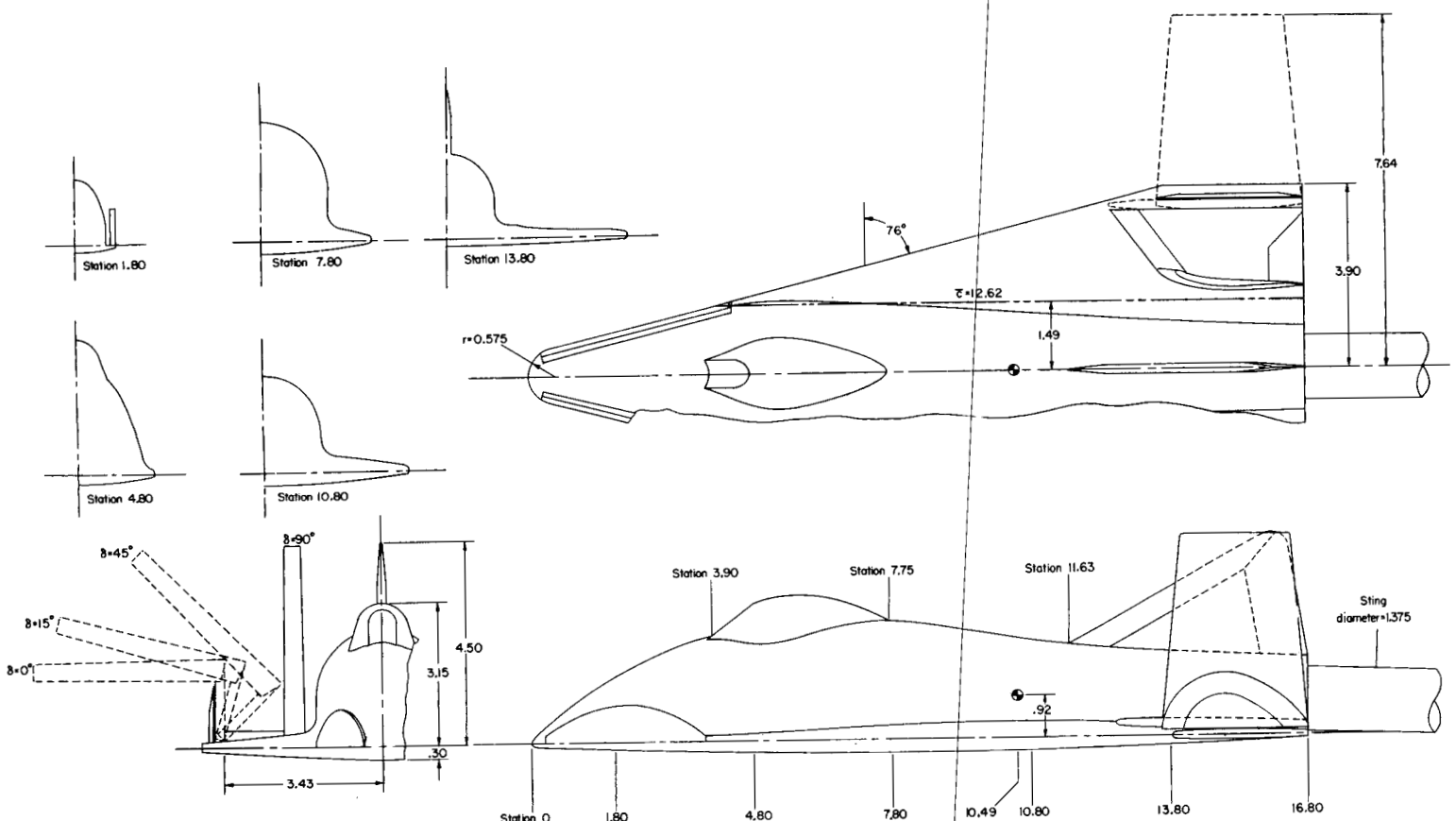

(a) Model on conventional sting.

Figure 1.- Details of model. All dimensions are in inches unless otherwise noted.

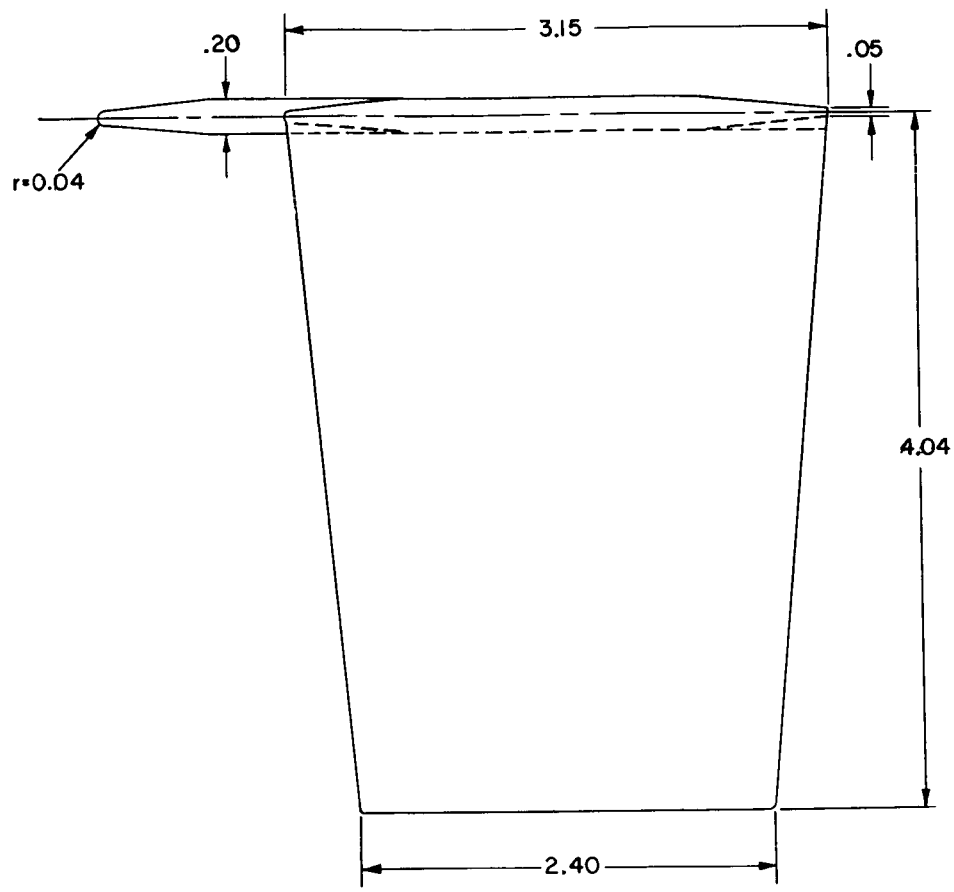

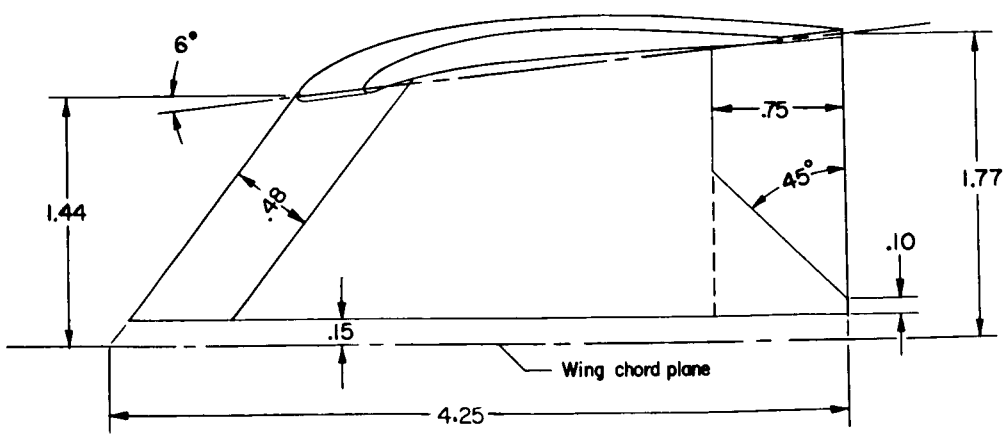

(b) Details of folding wing-tip panels.

Figure 1.- Continued.

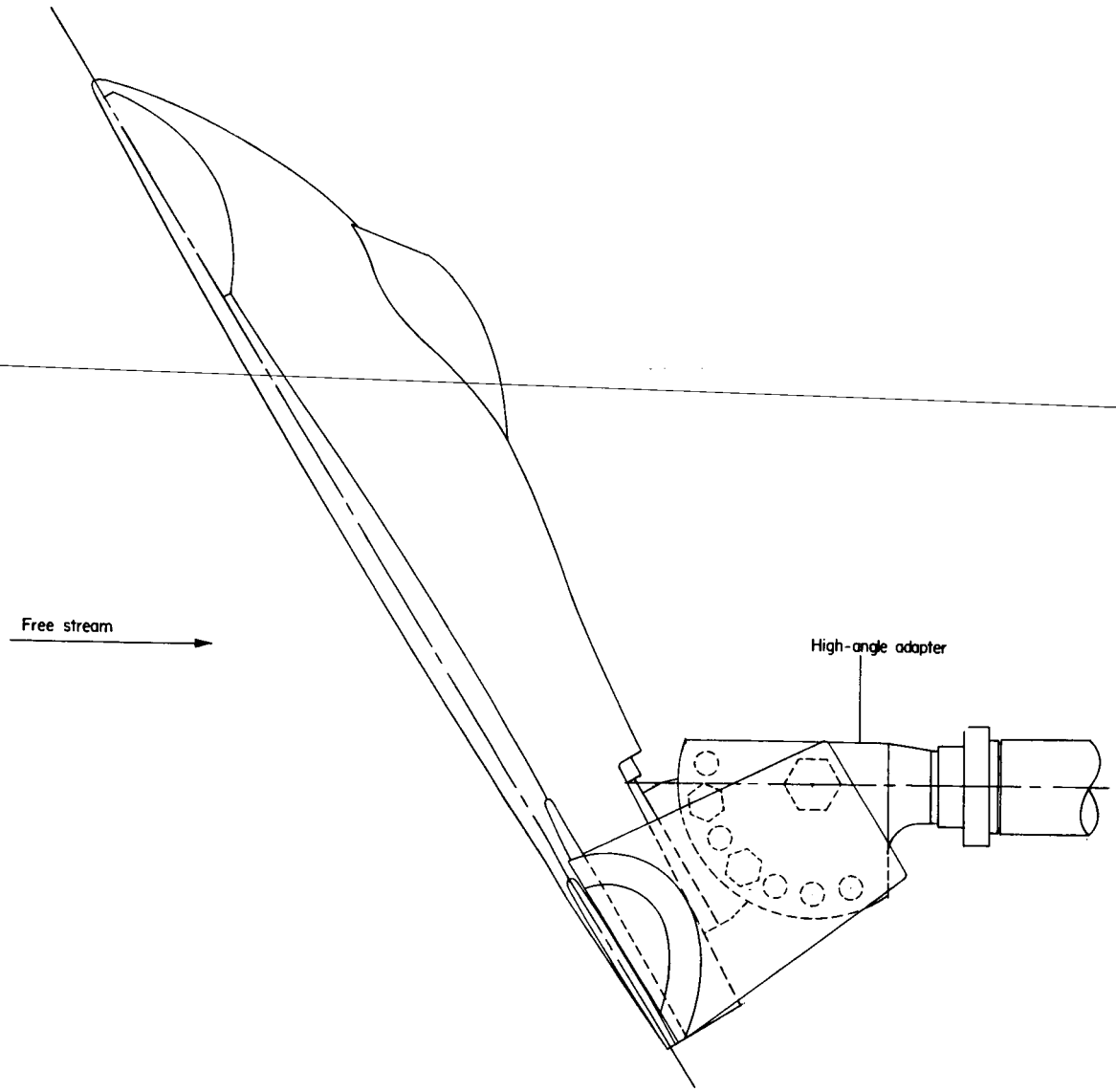

(c) Model on high-angle adapter.

Figure 1.- Concluded.

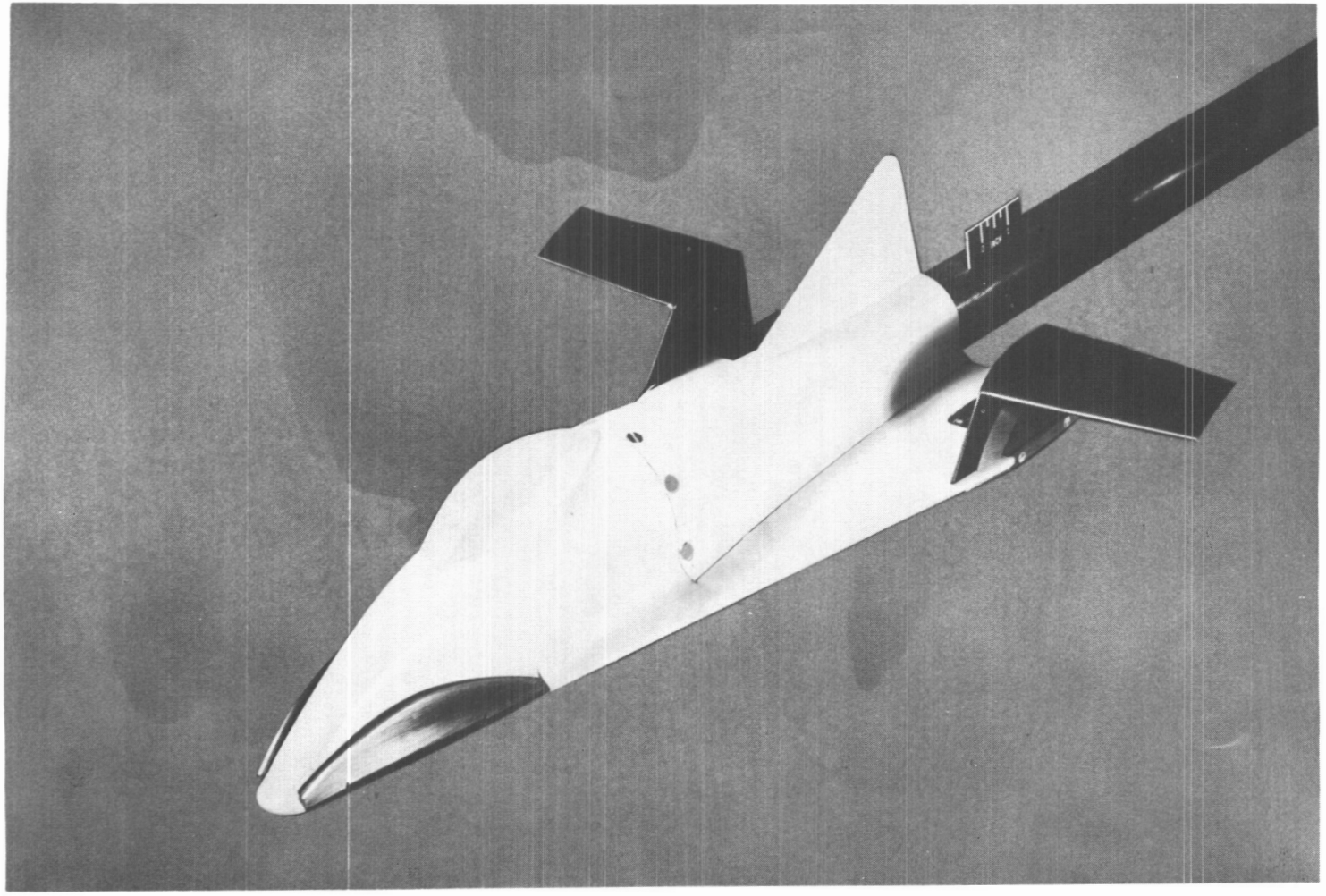

(a) Model on straight sting; $\delta = 0^{\circ}$. L-60-1627.1

Figure 2.- Photographs of model.

(b) Model on high-angle adapter. $\delta = 45^{\circ}$. L-60-1629.1

Figure 2.- Continued.

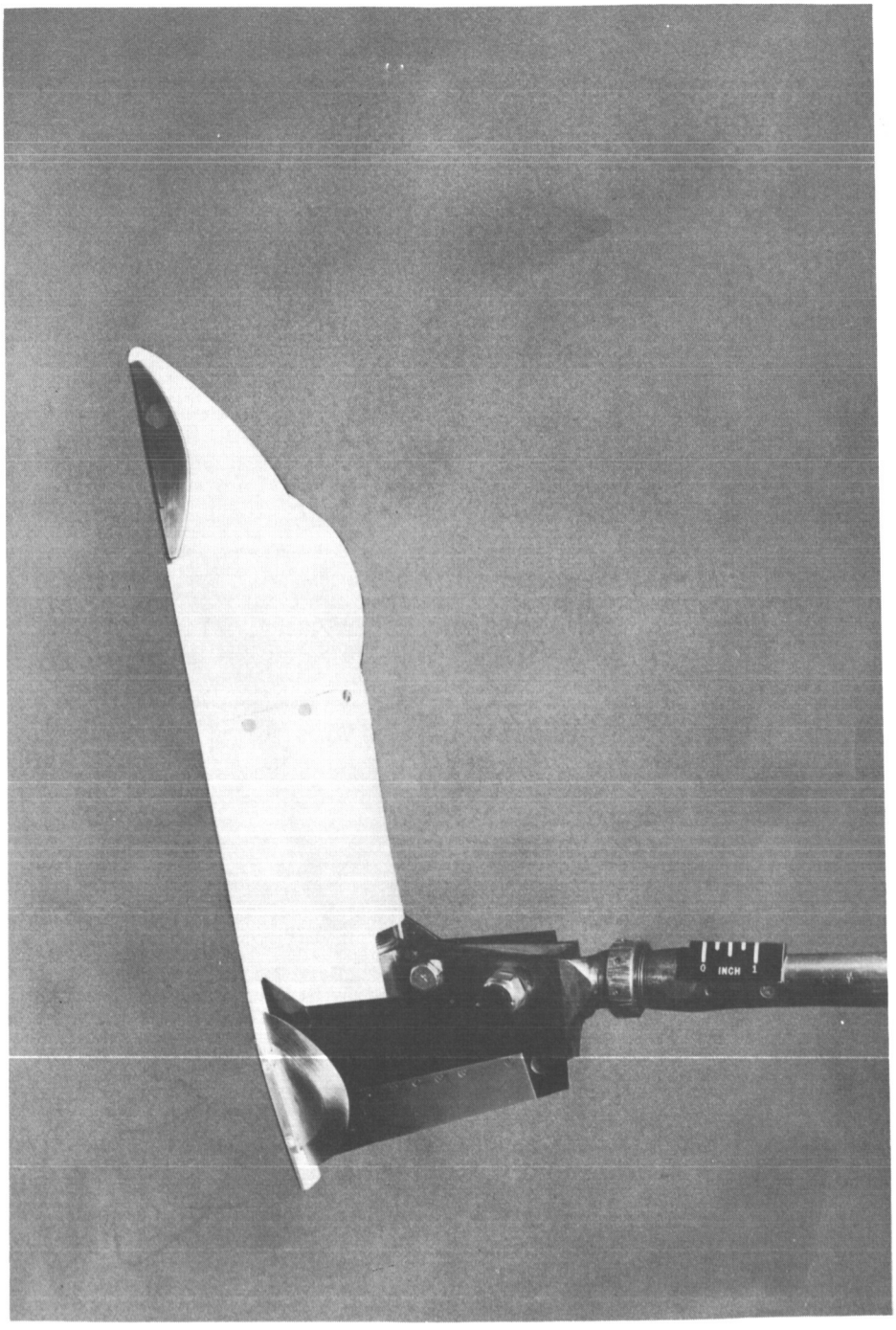

(c) Model on high-angle adapter; $\delta = 90^{\circ}$. L-60-1630.1

Figure 2.- Concluded.

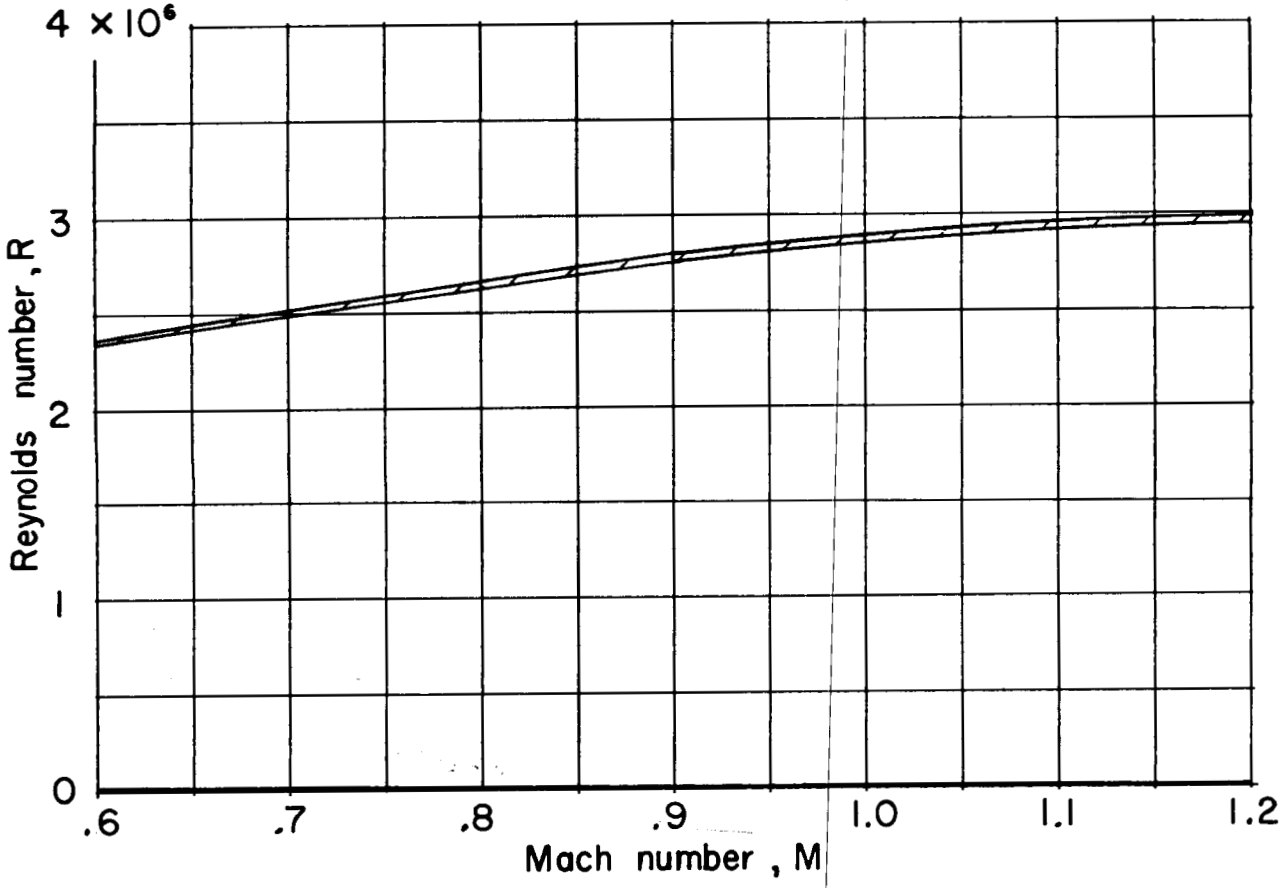

Figure 3.- Variation of Reynolds number range with Mach number. Reynolds number is based on the mean geometric chord of the fixed planform.

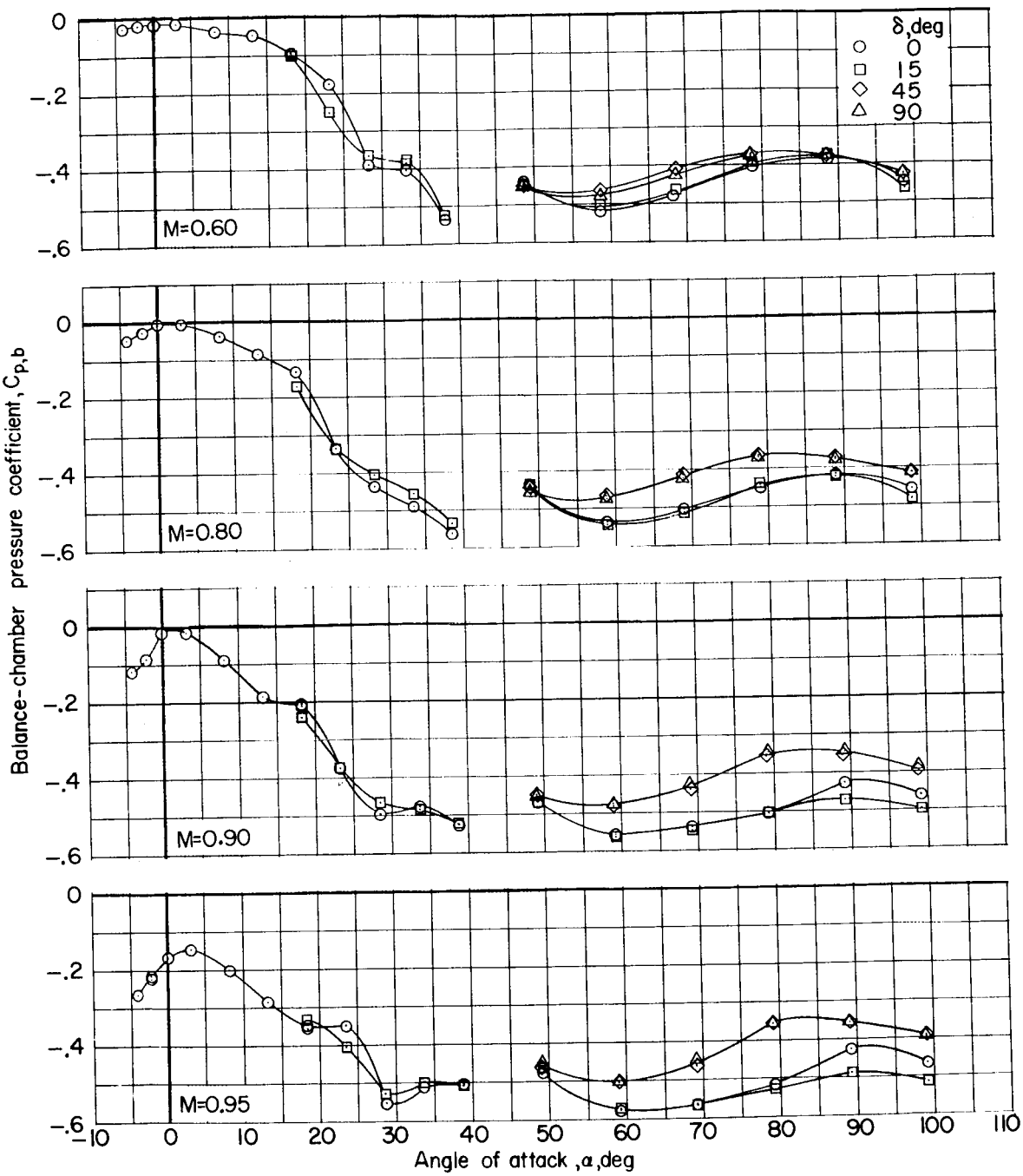

Figure 4.- Variation of balance-chamber pressure coefficient with angle of attack.

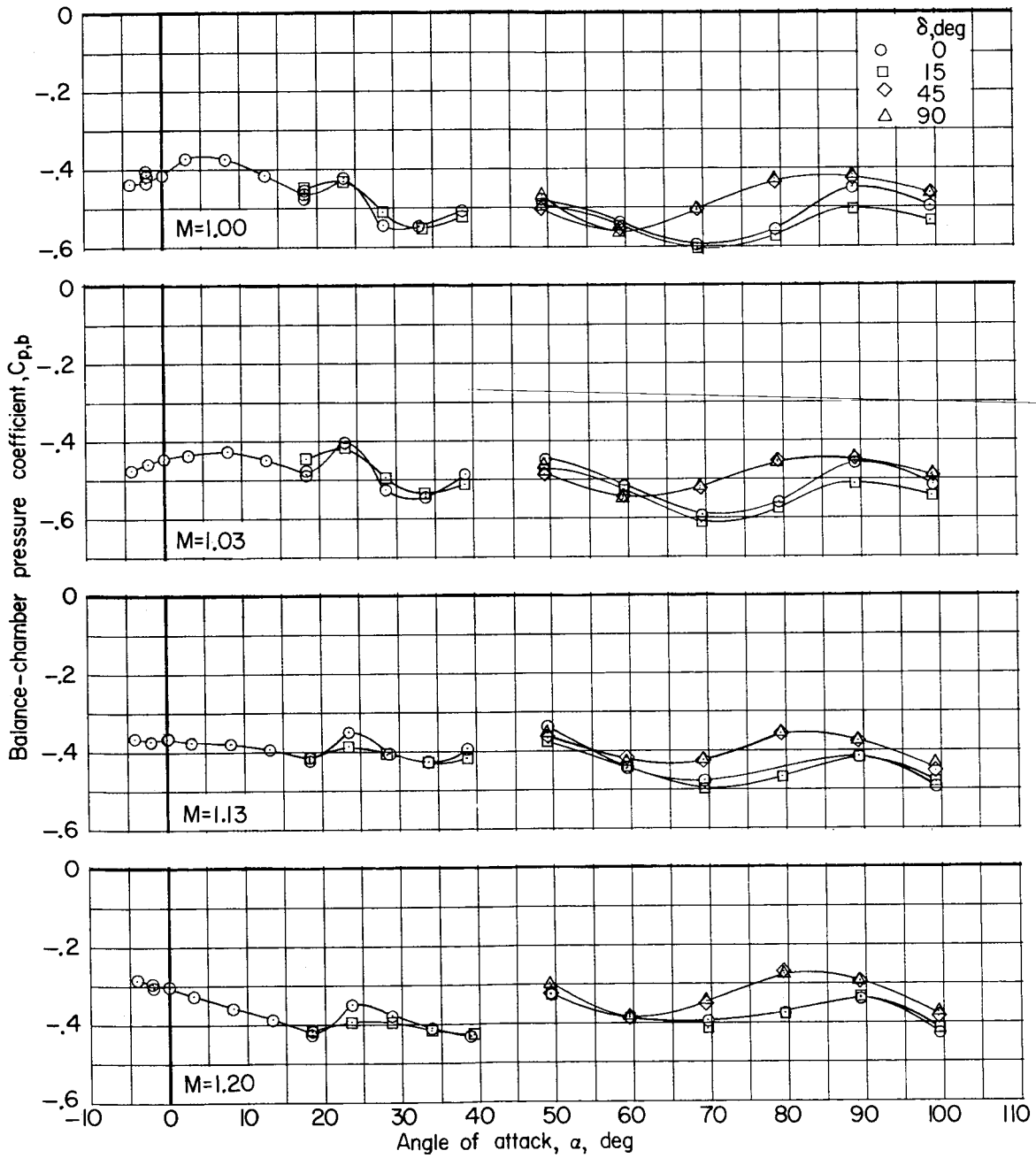

Figure 4.- Concluded.

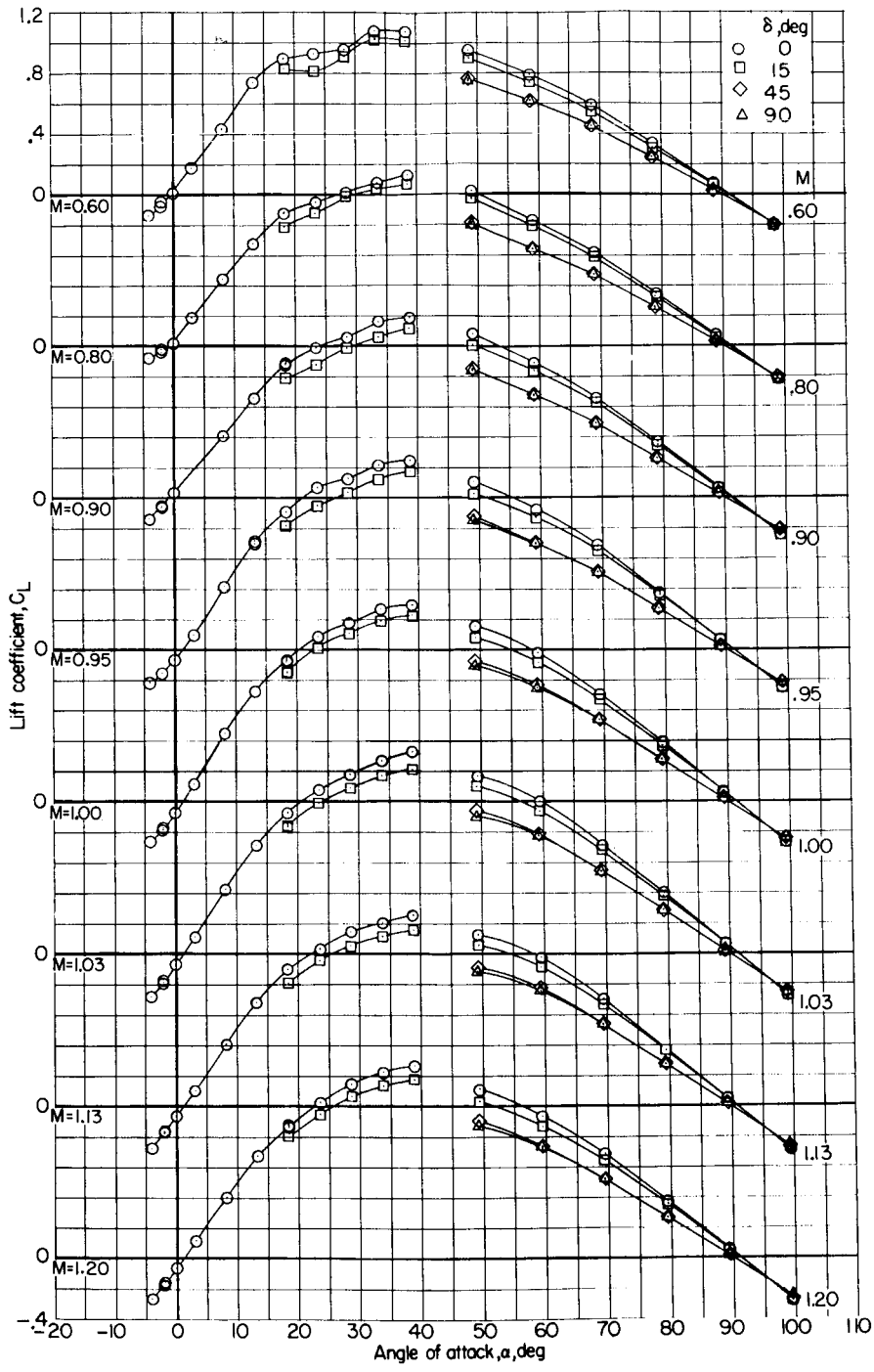

(a) Variation of lift coefficient with angle of attack

Figure 5.- Longitudinal aerodynamic characteristics of the model.

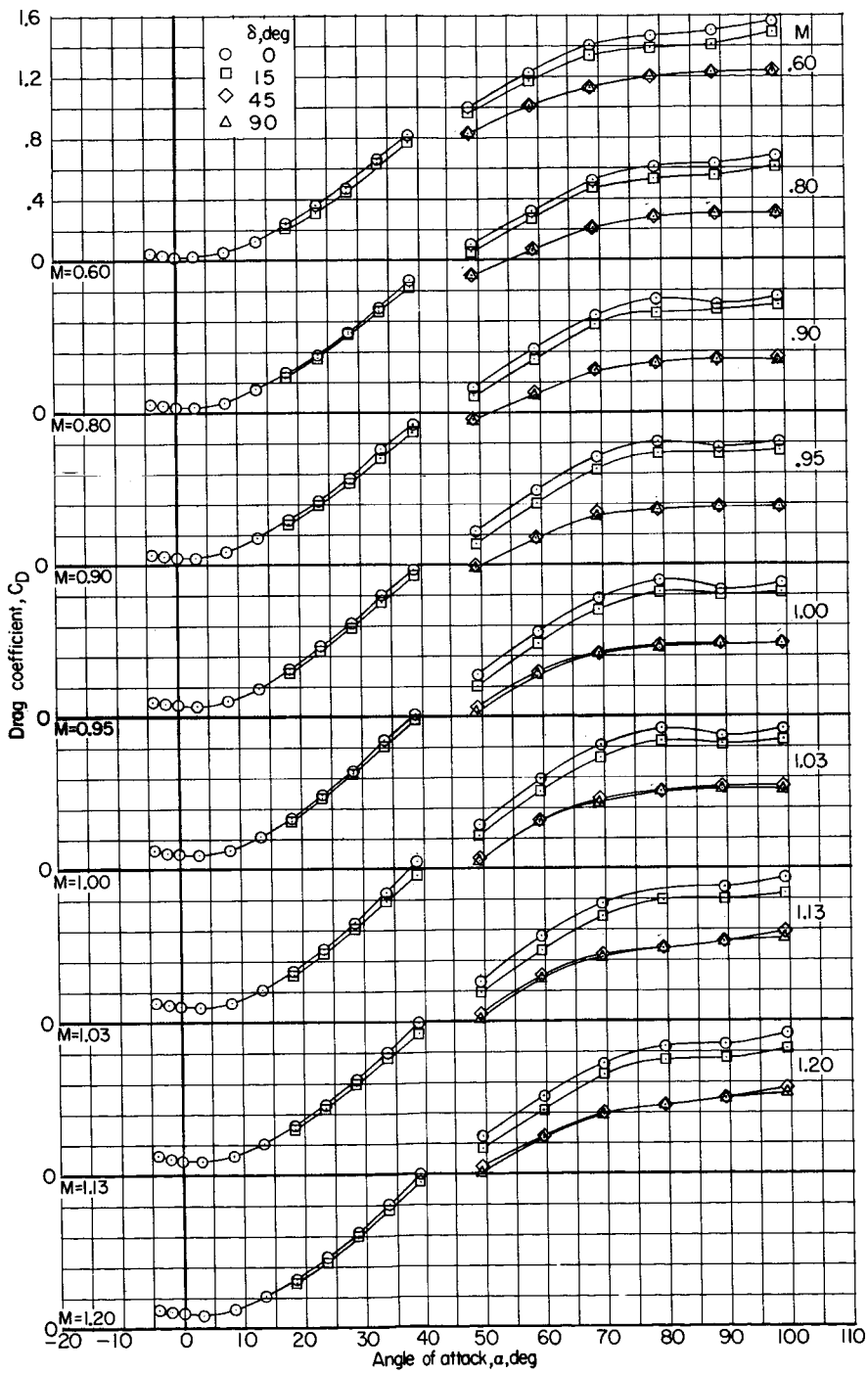

(b) Variation of drag coefficient with angle of attack.

Figure 5.- Continued.

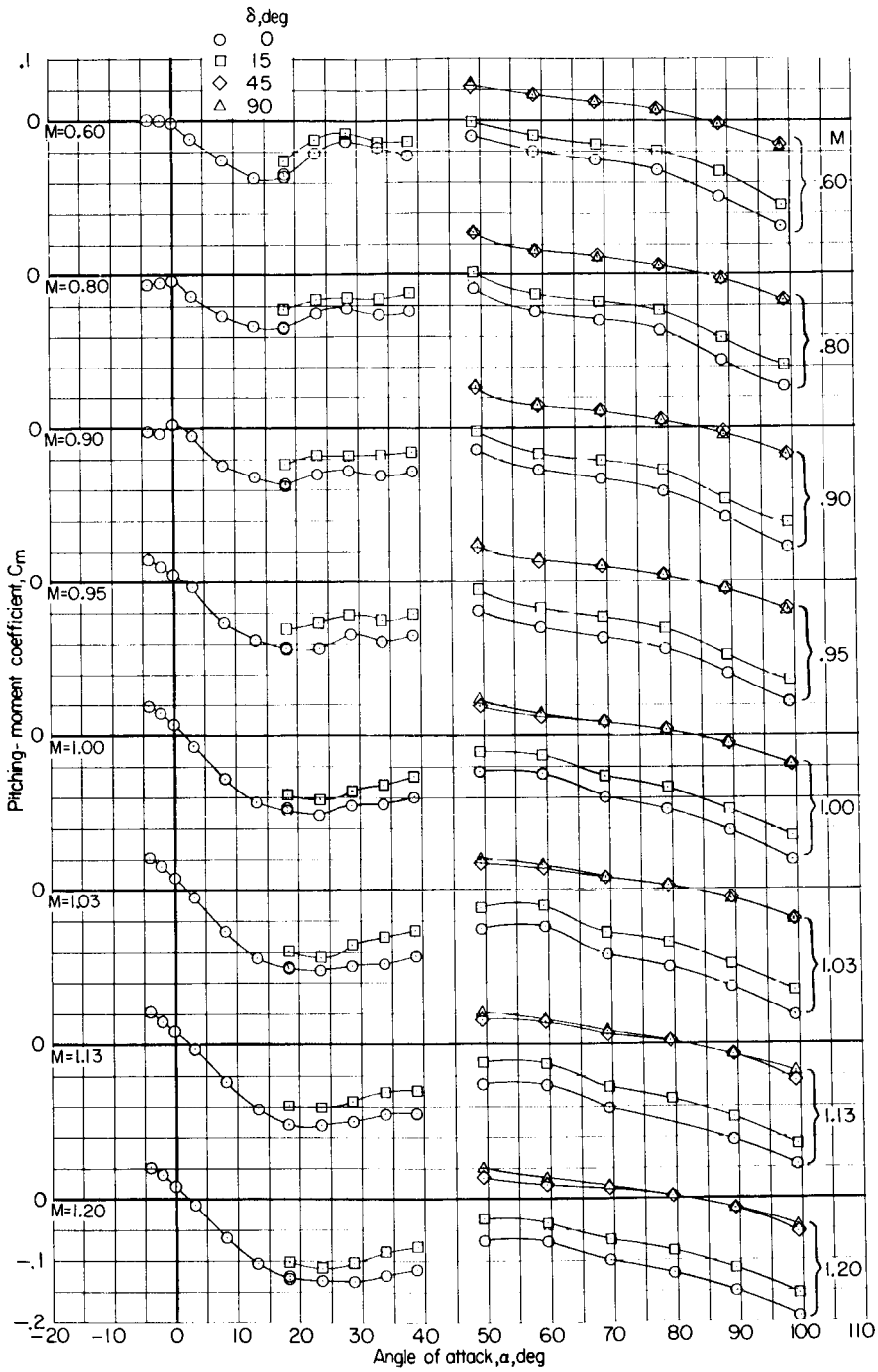

(c) Variation of pitching-moment coefficient with angle of attack.

Figure 5.- Continued.

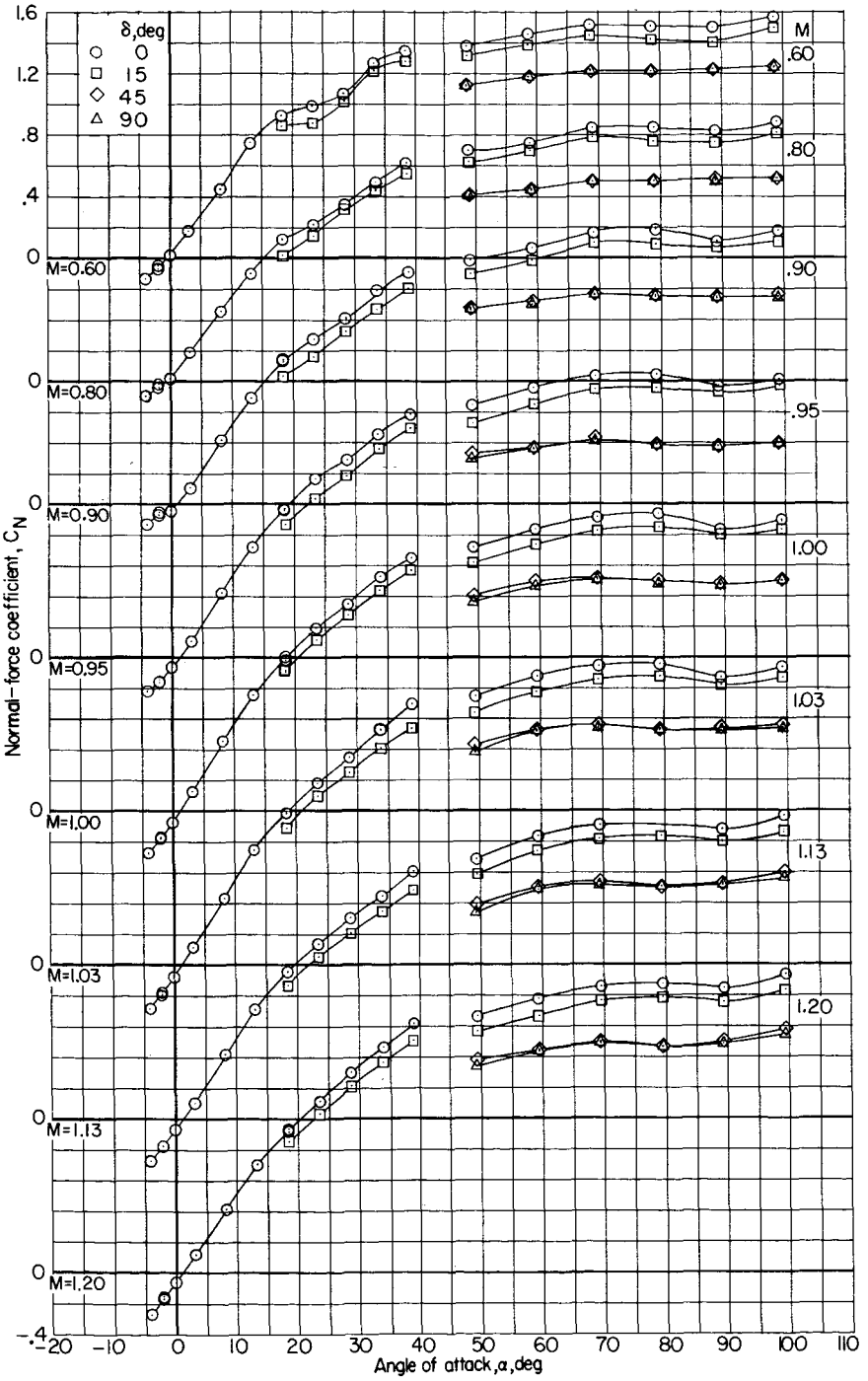

(d) Variation of normal-force coefficient with angle of attack.

Figure 5.- Continued.

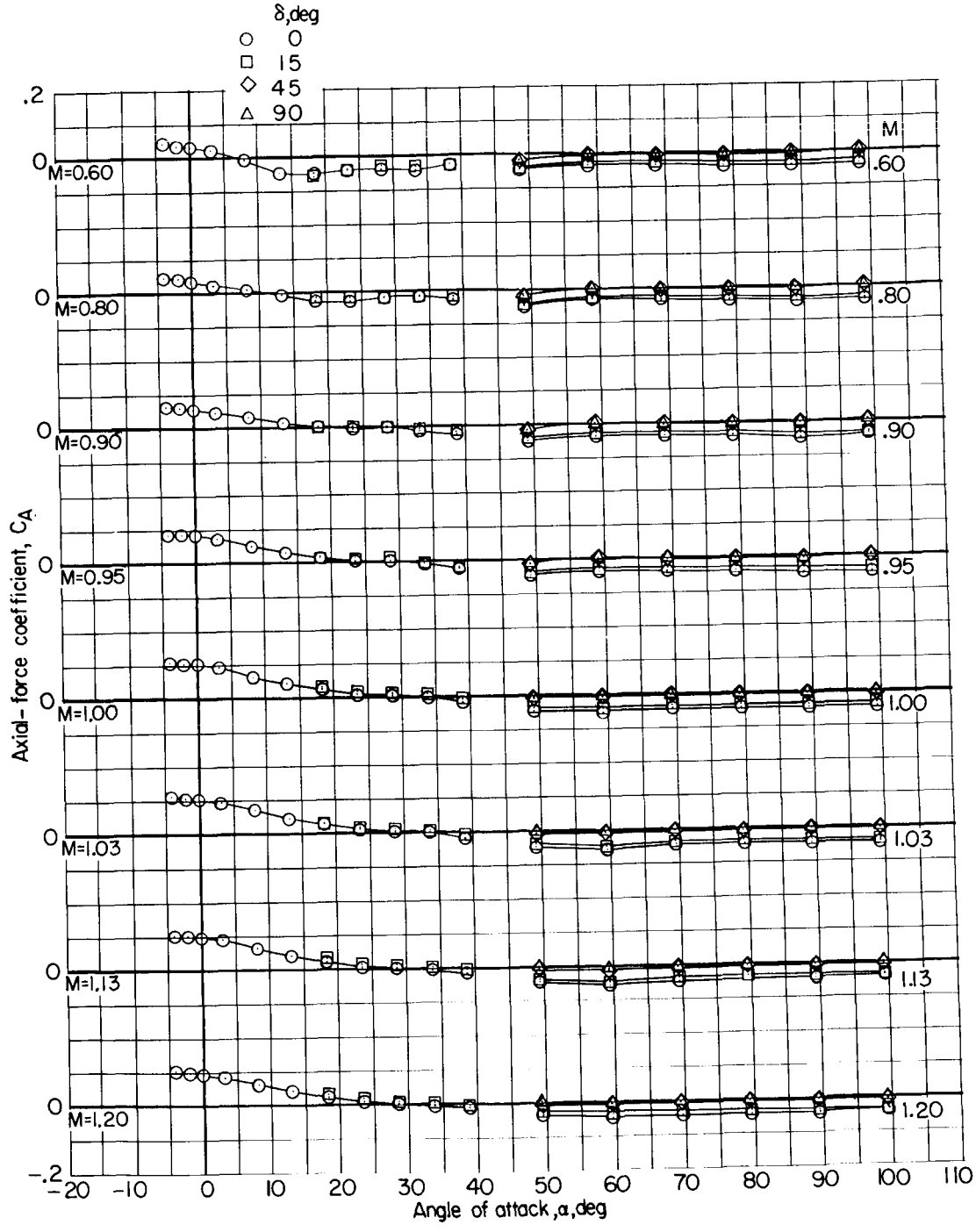

(e) Variation of axial-force coefficient with angle of attack.

Figure 5.- Continued.

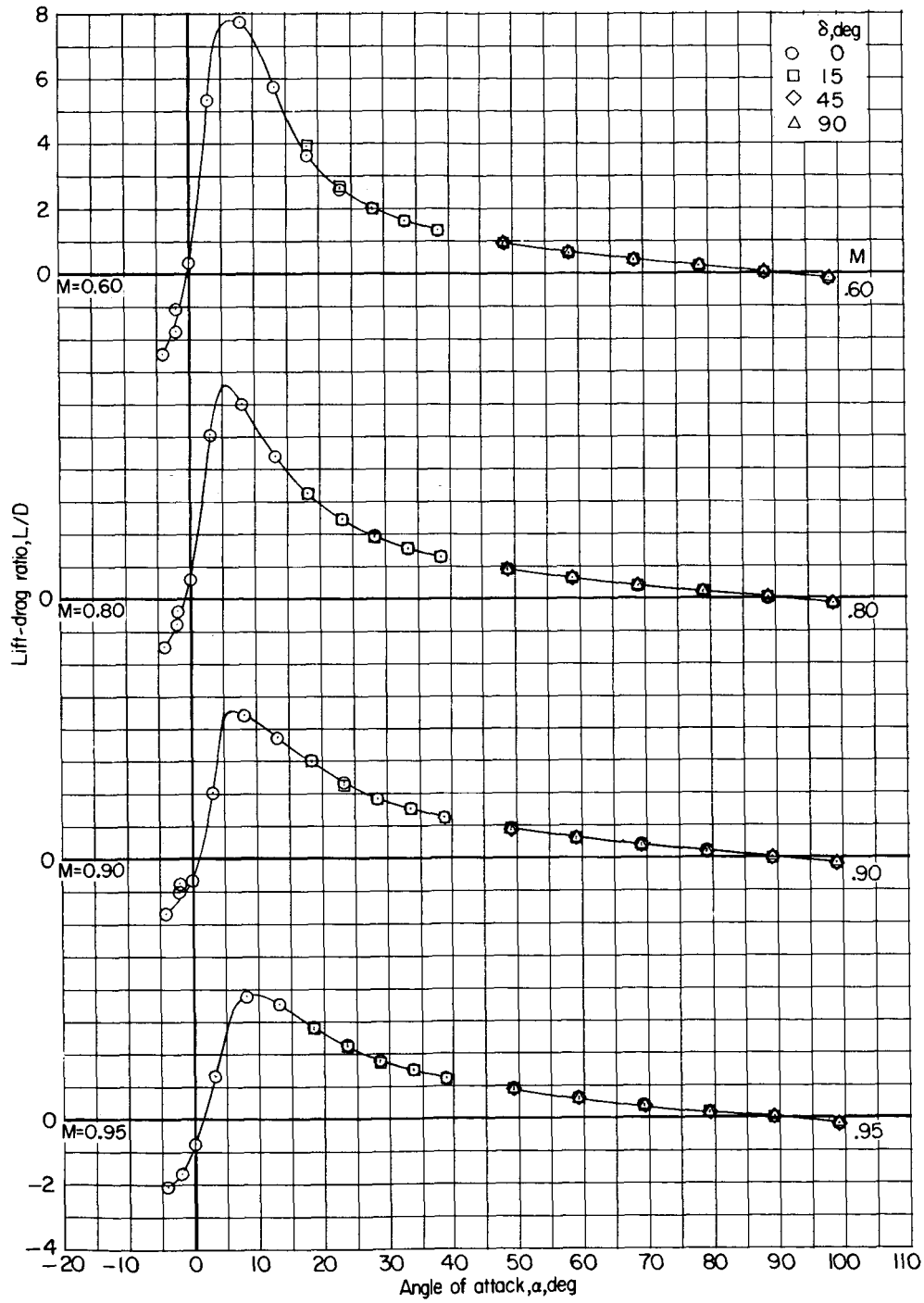

(f) Variation of lift-drag ratio with angle of attack.

Figure 5.- Continued.

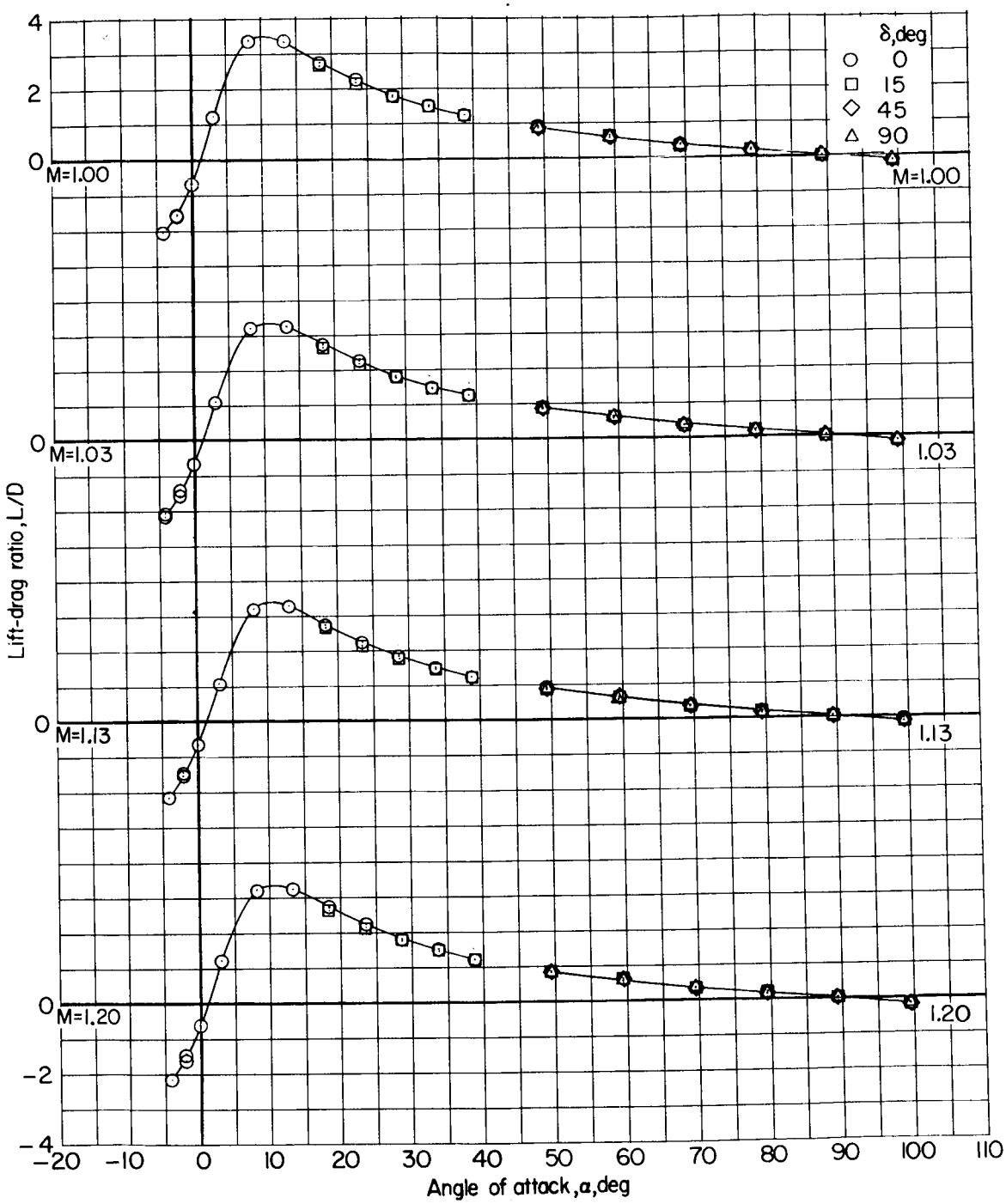

(f) Concluded.

Figure 5.- Concluded.

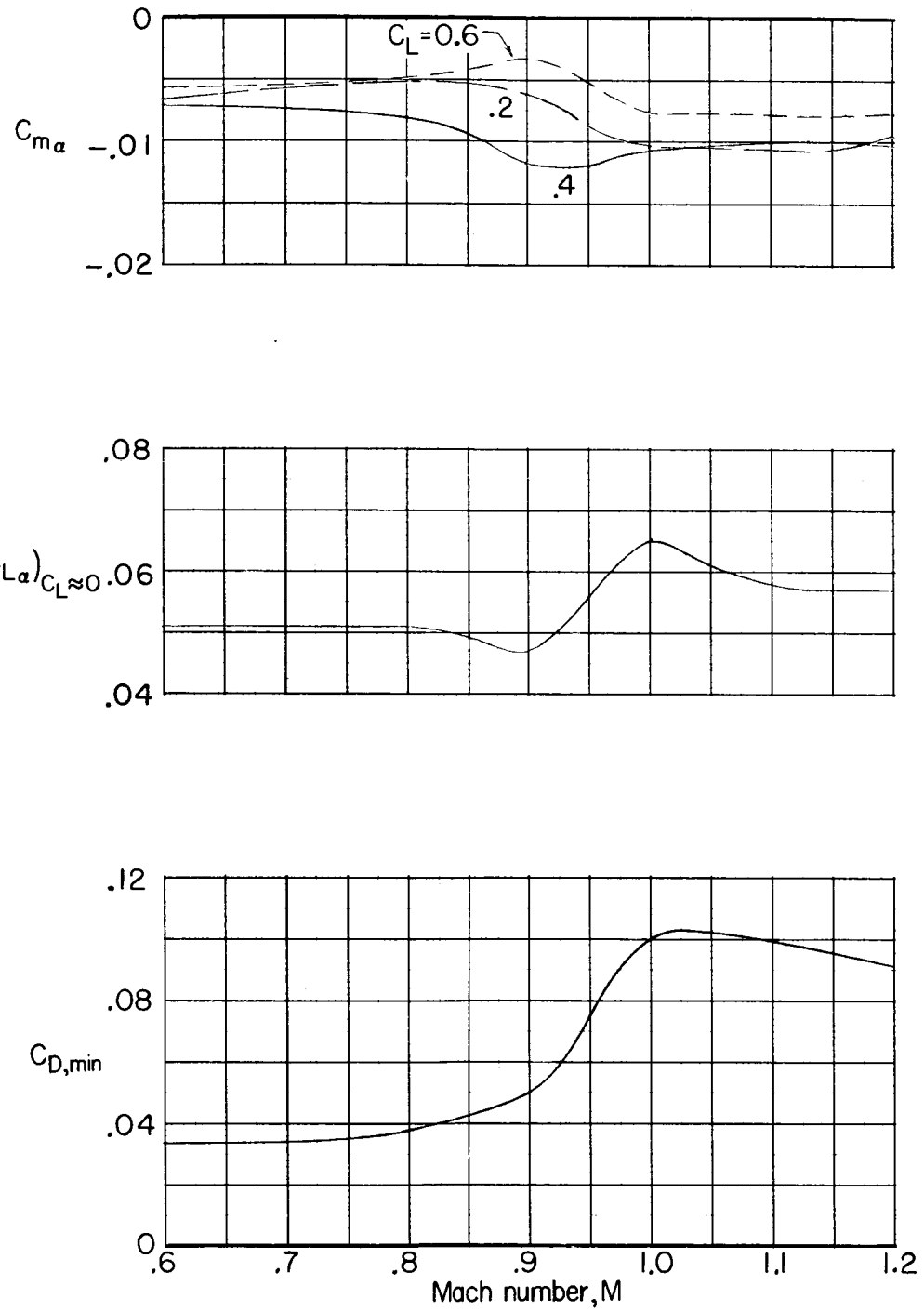

Figure 6.- Summary of longitudinal aerodynamic parameters at low angles of attack for the model with the folding wing panels fully extended ($\delta = 0^o$).

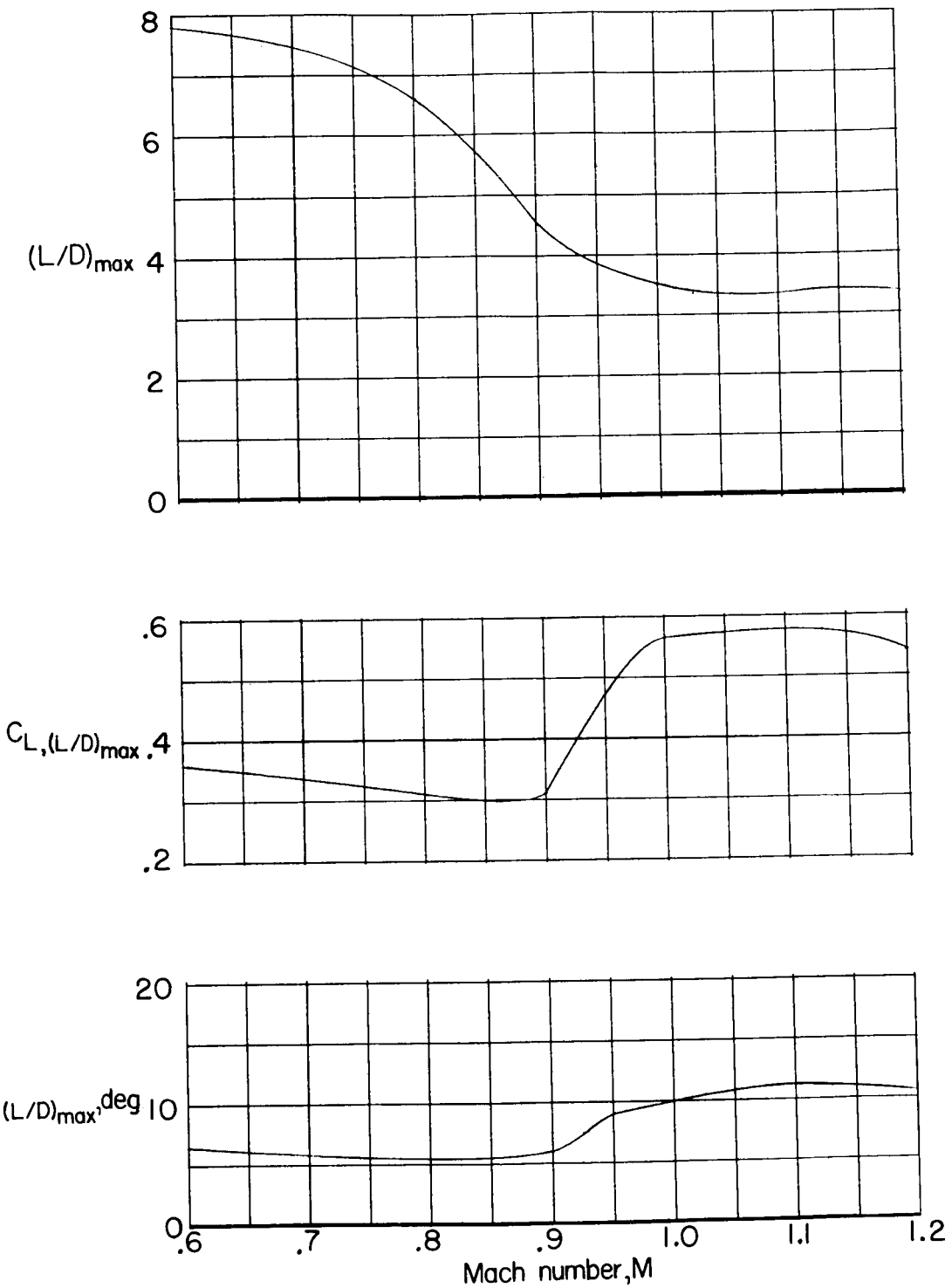

Figure 7.- Summary of characteristics for maximum lift-drag ratio for the model with the folding wing panels fully extended ($\delta = 0^{o}$).

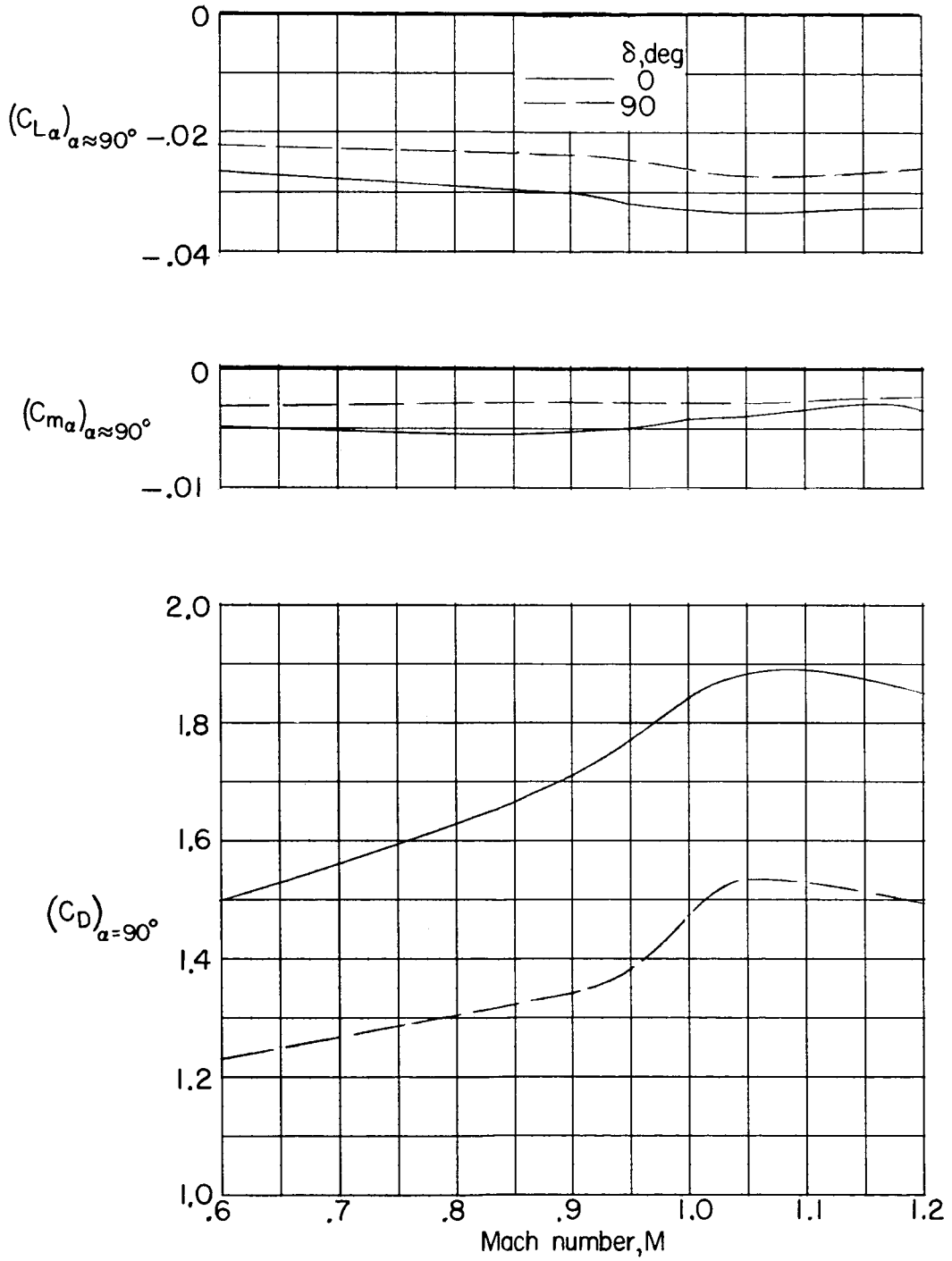

Figure 8.- Summary of longitudinal aerodynamic parameters near an angle of attack of 90° for the model with the folding wing panels fully extended (δ = 0°) and fully retracted (δ = 90°).